

Optical and electronic properties of fluorene/thiophene/benzothiadiazole pseudorandom copolymers for photovoltaic applications

Lucia Bonoldi · Anna Calabrese · Andrea Pellegrino · Nicola Perin · Riccardo Po · Silvia Spera · Alessandra Tacca

Received: 30 November 2010 / Accepted: 21 January 2011 / Published online: 5 February 2011
© Springer Science+Business Media, LLC 2011

Abstract A new family of 9,9-bisalkylfluorene (F)/thiophene (T)/benzothiadiazole (B) π -conjugated copolymers for organic solar cells is reported. The structure of the reported copolymers is pseudorandom: in turn each F, T, B monomer unit is alternated to the other randomly distributed two units. Voltammetric, UV-visible, and photoluminescence measurements have been carried out to assess the optical and electronic properties of the synthesized materials. The occurring of photoinduced charge transfer towards a fullerene electron acceptor was investigated by photoluminescence quenching and light-induced electron spin resonance experiments. The copolymer having alternating thiophene monomer units and randomly distributed fluorene and benzothiadiazole units exhibits the most promising characteristics; the photophysical study shows that such polymer/fullerene blend could represent a novel and cheaper material to be used as convenient donor–acceptor system for polymer solar cells.

Introduction

That of novel materials for new generation solar energy technologies is an expanding research area. In this frame,

polymer solar cells represent a hot topic and one of the most promising developments [1]. The achievement of efficient polymer solar cells requires a multidisciplinary research encompassing the synthesis of new π -conjugated systems, the photophysical characterization of the photoactive materials, the design, and fabrication of devices exhibiting nanostructured architectures, their electrical characterization and the study of the device physics. A large number of different donor and acceptor materials (both low molecular weight compounds and polymers) have been explored over the years [1–4] to find the best performing photoactive system. To date, the most active polymer solar cell, reaching a power conversion efficiency around 8% is based on a thieno[3,4-b]thiophene-benzo[1,2-b:4,5-b']dithiophene alternating copolymer [5–7] blended with a modified fullerene derivative.

It is possible, to some extent, to rationally design the structure of the donor polymer to tune its chemical, physical, and electronic properties which, in turn, affect the devices performance [8, 9]. Phenyl-C₆₁-butyric acid methyl ester (PCBM) and phenyl-C₇₁-butyric acid methyl ester are by far the most effective electron acceptors used in solar cells [1, 3]. For PCBM-based solar cells, it has been suggested that the energy gap of the donor should be in the range 1.5–1.8 eV and the LUMO (Lowest Unoccupied Molecular Orbital) level of the donor should be 0.3–0.5 eV above the LUMO level of PCBM [10]; on the other hand, no rational models have been developed to estimate, from the polymer structure or the photoactive blend morphology, the carrier mobility, another key parameter affecting the cell efficiency [4]. In general, conjugated copolymers containing electron rich/electron poor units in an alternate fashion are known to exhibit a low energy gap [11–18]. A class of promising materials with these characteristics is represented by the alternating

L. Bonoldi
Refining and Marketing Division Research Center,
ENI S.p.A, via Maritano 26, 20097 San Donato Milanese, Italy

A. Calabrese · A. Pellegrino · N. Perin · R. Po (✉) · S. Spera ·
A. Tacca
Research Center for non Conventional Energies Istituto Eni
Donegani, ENI S.p.A, Via Fauser 4, 28100 Novara, Italy
e-mail: riccardo.po@eni.com

A. Calabrese
Scuola Superiore di Catania, University of Catania, Via San
Nullo 5/I, 95123 Catania, Italy

fluorene copolymers (APFO) [2, 3, 19–29], which leads to solar cells having promising power conversion efficiencies. In particular, poly{9,9-bisalkylfluorene-2,7-diyl-*alt*-[4,7-bis(thien-2-yl)-2,1,3-benzothiadiazole]-5',5"-diyl} (alkyl = hexyl, 2-ethylhexyl, octyl, decyl, dodecyl), containing fluorene–thiophene–benzothiadiazole–thiophene units in a strictly alternating sequence [20, 21, 27, 29], exhibit energy gaps around 1.9 eV and open circuit voltages (V_{oc}) around 1 V.

In this study, we describe the synthesis and the optoelectronic characterization of a novel family of 9,9-bisalkylfluorene (F)/thiophene (T)/benzothiadiazole (B) pseudo-random copolymers.

Conjugated random copolymers [16, 19, 25, 30, 31] are, by far, less used than alternating copolymers for solar cells fabrication. While the disordered structure typical of the random polymers may hamper the crystallization and decrease the carrier mobility, the presence of different monomer units sequences might generate a plurality of energy gaps and increase the light harvesting ability.

An additional advantage of random copolymers over alternating copolymers consists in the simplicity of synthesis: while the preparation of alternating copolymers requires a multistep synthesis to assemble the monomeric units in the desired sequence, random copolymers can be easily obtained in a one-pot polymerization from readily available precursors.

Experimental

Materials

2,1,3-Benzothiadiazole-4,7-bis(4,4,5,5-tetramethyl)-1,3,2-dioxaborolane was purchased from Aldrich and purified by column chromatography (heptane/ethyl acetate 1:1). Toluene was distilled over lithium aluminium hydride.

9,9-Bis(2-ethylhexyl)fluorene-2,7-diboronic acid, 4,7-dibromo-2,1,3-benzothiadiazole, 2,7-dibromo-9,9-bis(2-ethylhexyl)fluorene, 2,5-dibromothiophene, tricaprylmethylammonium chloride (Aliquat® 336), palladium tetrakis(triphenylphosphine), methanol, isopropanol, chloroform, potassium carbonate, ethylenediaminetetraacetic acid disodium salt (EDTA), were purchased from Aldrich and used without further purification.

Polymerization procedure

Synthesis of poly{[4'-(9,9-bis(2-ethylhexyl)fluoren-2-yl)-2',1',3'-benzothiadiazole-7,7'-diyl]-co-[2'-(9,9-bis(2-ethylhexyl)fluoren-2-yl)thien-7,5'-diyl]} (**P1**). 1.736 g (3.63 mmol) of 9,9-bis(2-ethylhexyl)fluorene-2,7-diboronic acid, 533 mg (1.81 mmol) of 4,7-dibromo-2,1,3-benzothiadiazole and

439 mg (1.81 mmol) of 2,5-dibromothiophene were dissolved in a mixture of 40 mL of toluene and 8 mL of degassed isopropanol under nitrogen atmosphere. Five drops of Aliquat 336 and 4 mL of a 4 M (16 mmol) potassium carbonate in degassed water were added, and the mixture was heated to 70 °C for 15 min. 52 mg (0.040 mmol) of Pd(PPh₃)₄ were added and the reaction was carried out for 40 h under vigorous stirring. The reaction mixture was cooled, poured into 250 mL of methanol, and the coagulated solid was collected by filtration. The solid was redissolved in 500 mL of chloroform, 500 mL of 30% aqueous ammonia were added and the mixture was vigorously stirred for 3 h at reflux temperature. After cooling at room temperature the organic phase was separated, 400 mg of EDTA were added and the mixture was stirred overnight. Then the suspension was extracted three times with 500 mL of water. The organic phase was separated, concentrated to about 10 mL and added dropwise to 200 mL of methanol. The coagulated polymer was collected on a Gooch filter and dried in a vacuum oven to yield 1.702 g (94%) of a yellow-green powder.

Synthesis of poly{[2'-(thien-2-yl)-9',9'-bis(2-ethylhexyl)fluorene-5,7'-diyl]-co-[4'-(thien-2-yl)-2',1',3'-benzothiadiazole-5,7'-diyl]} (**P2**). 627 mg (1.40 mmol) of 9,9-bis(2-ethylhexyl)fluorene-2,7-diboronic acid, 545 mg (1.40 mmol) of 2,1,3-benzothiadiazole-4,7-bis(4,4,5,5-tetramethyl)-1,3,2-dioxaborolane, and 680 mg (2.81 mmol) of 2,5-dibromothiophene were polymerized following the same procedure described for **P1**. 472 mg (49%) of a dark brown powder were obtained.

Synthesis of poly{[2'-(2,1,3-benzothiadiazole-4-yl)-9',9'-bis(2-ethylhexyl)fluorene-7,7'-diyl]-co-[2'-(2,1,3-benzothiadiazole-4-yl)thien-7,5'-diyl]} (**P3**). 873 mg (1.59 mmol) of 2,7-dibromo-9,9-bis(2-ethylhexyl)fluorene, 1.239 g (3.19 mmol) of 2,1,3-benzothiadiazole-4,7-bis(4,4,5,5-tetramethyl)-1,3,2-dioxaborolane, and 385 mg (1.59 mmol) of 2,5-dibromothiophene were polymerized following the same procedure described for **P1**. 817 mg (70%) of a dark brown powder were obtained.

Characterization methods

UV–Vis absorption spectra were recorded at room temperature with a Lambda 950 spectrophotometer (PerkinElmer Inc. Waltham, MA, USA). Samples in solution were prepared by dissolving pristine polymer in CHCl₃ solutions in cell with 10 mm optical path length and optical density of typically 0.5 at max. absorption in the visible region of spectrum. Thin films (~100 nm) of pristine polymers and polymer/PCBM blends were prepared by spin-coating from chlorobenzene solution on quartz Suprasil substrates. The optical energy gaps were evaluated by the edge corresponding to the intersection between the negative tangent

line in the inflection point of lowest energy absorption band and the tangent line to linear portion of the absorption tail.

Steady-state PL spectra were recorded at room temperature with a Fluorolog 3 spectrofluorometer (Horiba Jobin-Yvon Inc., Edison, NJ, USA), with right angle geometry for liquid samples and front-face (22°) for thin films. The same samples used for absorption was used for PL quenching measurement; emission spectra were corrected for the optical density of the sample at the excitation wavelength.

Electrochemical measurements were performed with an Autolab PGSTAT30 potentiostat/galvanostat (EcoChemie, The Netherlands) run by a PC with GPES software, in a one-compartment three-electrode cell in argon-purged acetonitrile with 0.1 M Bu_4NBF_4 as supporting electrolyte. A CHCl_3 solution 1 mg/mL of the compound was coated on the Glassy Carbon working electrode (Amel Electrochemistry, Milano, Italy) having a surface of 0.071 cm^2 . A Platinum counterelectrode and an aqueous saturated calomel (SCE) reference electrode were used. The film formed on the electrode was analysed at a scan rate of 200 mV/s. The data have been referred to the Fc^+/Fc redox couple (ferricinium/ferrocene), according to IUPAC [32].

NMR spectra were obtained with an Avance 400 spectrometer (Bruker Corp., Madison, WI, USA). Samples were dissolved in CDCl_3 (reference: 7.26 ppm for ^1H and 77.7 ppm for ^{13}C). ^1H -NMR spectra were acquired with a 90° pulse width and 4 s as delay time. $^{13}\text{C}[^1\text{H}]$ -NMR spectra were acquired with 30° pulse width and 2 s as delay time.

The Light-induced Electron Spin Resonance (LESR) measurements were performed with a Bruker Elexys 500 spectrometer, equipped with a nitrogen flow cryostat. Thick film (estimated thickness $20 \mu\text{m}$) were casted inside the sample holder quartz tube, after three freeze–pump–thaw cycles of the sonicated Cl-benzene solutions of pure polymer or polymer/PCBM 1:1 w/w mix, in order to eliminate at best oxygen traces. After a prolonged (2 h) vacuum treatment the ESR spectra were registered at 120 K in absence (“dark” spectrum) and presence of illumination (“light” spectrum). Light is irradiated through a 66% transmission grid on the resonant cavity from a 1,000 W high pressure Xenon lamp with a water filter ($\approx 2 \text{ mW/cm}^2$ in non-focussed conditions), chosen in order to simulate solar spectrum irradiation. The difference “light”–“dark” is the LESR, where the presence of the signals of polaron $\text{P}^{\pm\circ}$ and $\text{PCBM}^{\pm\circ}$ shows the occurrence of the photoexcited charge transfer [33]. Microwave power scans were performed in order to find the conditions (0.05 mW microwave power) to avoid polaron signal saturation, generally occurring at relatively low power in both poly(3-alkylthiophene)s [34], and poly(9,9-diptylfluorene) [35] reference derivatives.

Molecular weight determinations were made using a Waters 150C chromatograph (Waters Corp. Milford, MA,

USA) equipped with a refractive index detector on 1,2,4-trichlorobenzene solutions at 80°C . Molecular weight calibration was performed using monodisperse polystyrene standards.

Results and discussion

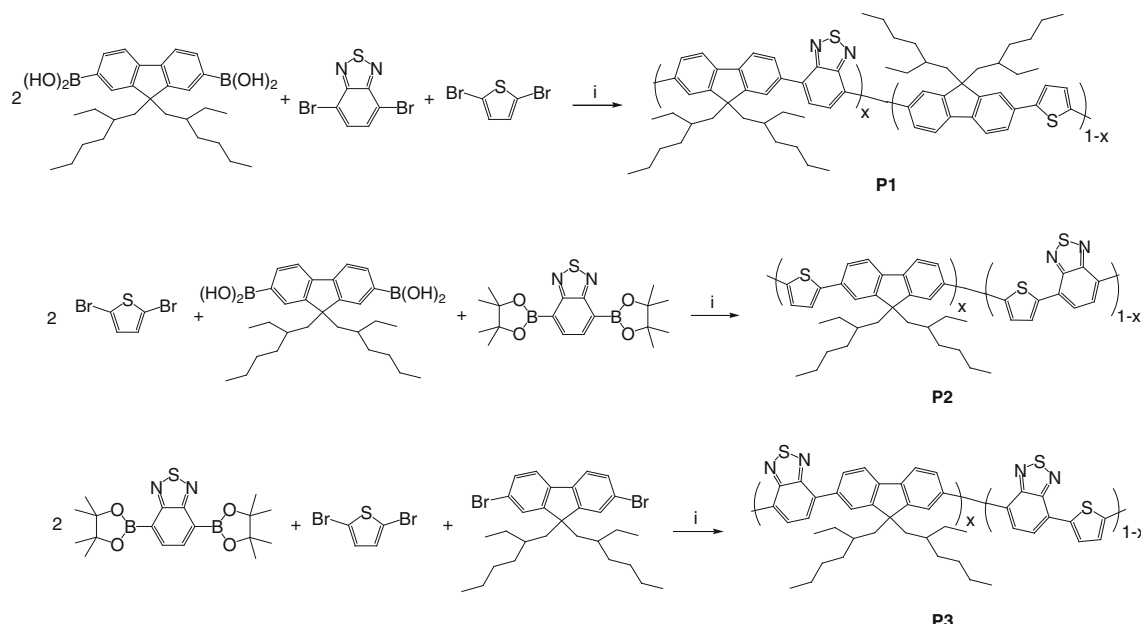
Fluorene/thiophene/benzothiadiazole pseudo-random copolymers were synthesized by Suzuki cross-coupling polymerization [36] from dibromides and boronic diacids or diesters, according to Scheme 1.

As a result of the adopted procedure, in the three copolymers in turn each F, T, B comonomer unit is alternated to the other two units, which are randomly distributed (Scheme 2).

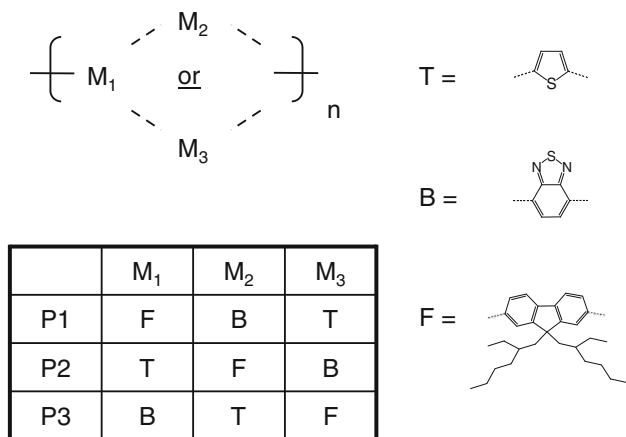
P1 and **P3** were obtained from 9,9-bis(2-ethylhexyl)fluorene-2,7-diboronic acid and 2,1,3-benzothiadiazole-4,7-bis(4,4,5,5-tetramethyl)-1,3,2-dioxaborolane, respectively, reacted with an equimolar mixture of the complementary dibromides. The synthesis of **P2** from thiophene-2,5-diboronic acid and a 1:1 mixture of 2,7-dibromo-9,9-bis(2-ethylhexyl)fluorene and 4,7-dibromo-2,1,3-benzothiadiazole was also attempted, but no polymer was recovered. A possible explanation for this might be that deboronation side-reaction prevents the aryl–aryl coupling and the polymerization [37, 38]. This problem was already observed before in the case of polymerization with thiophene-2,5-diboronic acid as starting monomer [39, 40]. Thus, **P2** was prepared from 2,5-dibromothiophene and an equimolar mixture of boronic derivatives of the two other comonomers, affording a dark brown product in fairly good yield.

According to the literature [20, 41, 42], F–T–B–T alternating copolymer obtained by Suzuki polymerization has a relatively low molecular weight ($M_w < 15,000$) as compared to other fluorene copolymers. The reason for that was attributed to the low solubility arising from the limited number of alkylated aromatic rings in the backbone: the high molecular weight portion of the product tends to remain in the insoluble fraction of the product. Among the examined polymers, **P1** contains the greater number of alkylated units, thus is the more soluble polymer and hence the one exhibiting the higher molecular weight ($M_w = 34,600$). On the opposite, **P3** is the less soluble polymer, with a marked tendency to aggregate. For this reason, the study here reported and the measurements have been carried out for the series **P1**–**P3**, but in the following only **P1** and **P2** are discussed, because **P3** in most cases have broad and poorly defined spectra.

Special care was paid to the products purification to remove catalyst residues. A simple reprecipitation step, a procedure often applied in the literature, leaves into the



Scheme 1 Synthesis of **P1**, **P2**, and **P3**. Reaction conditions: toluene/ROH/water, K_2CO_3 , Aliquat 336, $Pd(PPh_3)_4$, $70\text{ }^\circ C$, 40 h



Scheme 2 Structure of fluorene/thiophene/benzothiadiazole pseudo-random copolymers

final product high levels of palladium ($>1,000$ ppm) and phosphorus (800–9,000 ppm) impurities. The purity of the polymer is important, as metal residues might act as charge traps and affect the electrical properties [43, 44]. By treating the organic solution of the polymer with ammonia and EDTA solutions [45, 46], as described in the experimental part, it was possible to decrease the palladium concentration in **P1** and **P2** by more than one order of magnitude (i.e., to less than 100 ppm). On the opposite, phosphorous concentration remains high, at around 800 ppm. In any case, as a side result of the present study it has been shown that through an appropriate procedure it is possible to greatly reduce the residual metal content in this class of materials.

A detailed study of the polymers microstructure and monomer sequence distribution by NMR and FT-Raman is currently under way and will be published elsewhere. In this study, only the monomer composition is reported. The experimental compositions of **P1** and **P2** determined by nuclear magnetic resonance are near to the nominal ratio expected on the basis of the monomers feed (Table 1: $x \sim y \approx 0.5$); the discrepancies arise from the partial overlapping of some peaks. For **P1** the experimental F:T:B monomer ratio is 0.47:0.27:0.25, while for **P2** is 0.28:0.51:0.21 (the accuracy is estimated around $\pm 5\%$).

UV-visible absorption spectra of **P1** and **P2** solid films are reported in Fig. 1. In addition, absorptions were measured also in chloroform solution; blue-shifts (15–25 nm) were observed in solution compared to the films, suggesting that in the latter cases significant solid intermolecular interactions exist [47].

P1 ((FT) $_x$ -co-(FB) $_y$) contains long electron rich F-T sequences interrupted by B electron poor units; on average, there are 4.75 electron rich rings (in the calculations fluorene counts for two rings) for any electron poor group. In other words, electron poor units are somewhat too sporadic along the chain to lead to a low bandgap structure [11–13]. Furthermore, F-B linkages causes a rotation around the

Table 1 Molecular weight, molecular weight distribution, and optical properties of **P1** and **P2**

Entry	Structure	M_W (Da)	M_W/M_n	$E_{g(\text{opt})}$ (eV)	λ_{max} (nm)
P1	(FT) $_x$ -co-(FB) $_y$	34,600	3.0	2.38	459
P2	(TB) $_x$ -co-(TF) $_y$	3,200	1.8	1.86	551

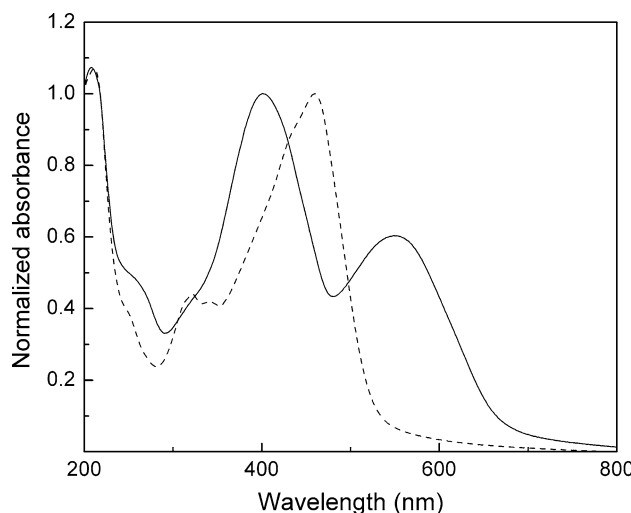


Fig. 1 Absorption spectra of films of random copolymers **P1** (solid curve) and **P2** (dash curve) normalized at the band around 400 nm

aryl–aryl bond for steric reasons and hence a loss of planarity and conjugation. Accordingly, in spite of its high molecular weight **P1** exhibits an absorption peak at 459 nm, the lowest value in this class of polymers, and an absorption edge at 522 nm, corresponding to an optical gap of 2.38 eV.

For comparison, the UV–visible spectra of F–T and F–B alternating binary copolymers (Scheme 3) in chloroform solution were also registered. The spectrum of F–B (Fig. 2a) shows two absorption peaks centered at 319 and 431 nm, which can be attributed to a $\pi-\pi^*$ and intrachain charge transfer (iCT) transition, respectively [48]; on the other hand, F–T exhibits a single absorption at 442 nm due to $\pi-\pi^*$ transition. Interestingly, from Fig. 2b it can be seen that the spectrum of **P1** in CHCl_3 solution is quite well approximated by a linear combination of the spectra of F–T and F–B ($A(\lambda)_{\text{P1}} = A(\lambda)_{\text{F-T}} + k * A(\lambda)_{\text{F-B}}$) (k is a constant dependent on molar absorptivity of F–T and F–B polymers and relative abundance of corresponding co-monomers in **P1**). Apparently, the iCT band of the F–B portion at 431 nm of **P1** is totally hidden by the $\pi-\pi^*$ band attributed to the F–T sequences. Still, the fact that the ternary random copolymer appears to be a combination of the two parent binary copolymers suggests that the conjugation of the

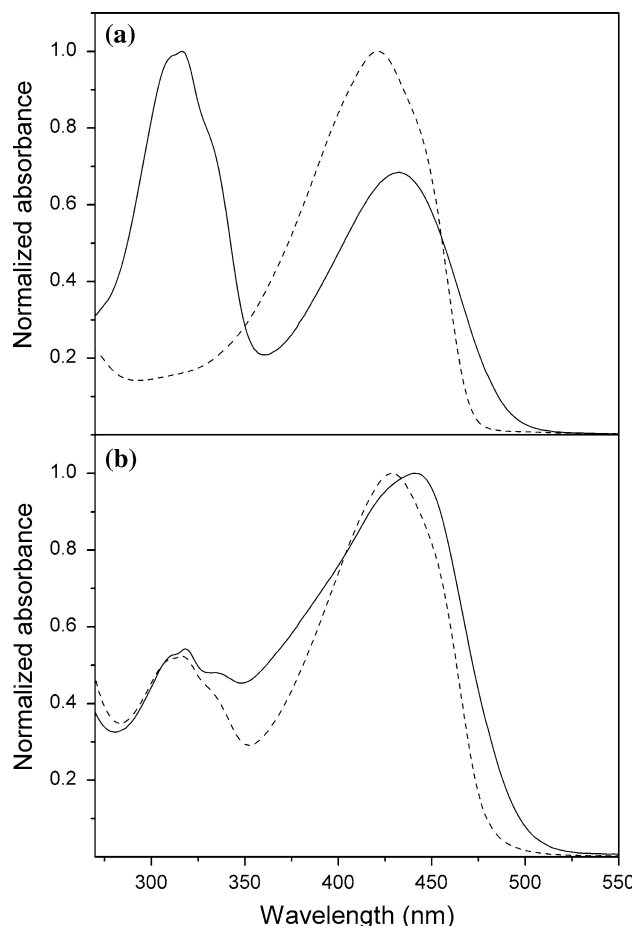
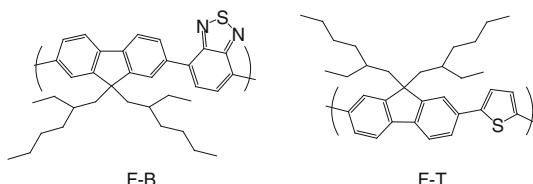


Fig. 2 **a** Experimental UV–vis spectrum of F–B (solid curve) and F–T (dash curve) alternating copolymers in chloroform solution and **b** experimental spectrum of **P1** (solid curve) compared to linear combination of F–B and F–T spectra (dash curve)

molecular chain is imperfect, otherwise the resulting delocalized system would exhibit very different features, with significant shifts in the peak positions.

F–T–B–T alternating polymers have a characteristic “camel back”-shaped absorption [25, 29]. When the $(\text{TB})_x$ -co-(TF)_y random copolymer (**P2**) is compared to F–T–B–T one can observe the same spectroscopic features. However, while the red band and the blue band of the alternating copolymers are equal in intensity [25], in **P2** the blue band is much more intense than the red one (Fig. 1). Moreover, the blue band (associated to a delocalized excitonic $\pi-\pi^*$ transition showing exchange of double and single bonds) of the random copolymer is broader and slightly red-shifted: it can be speculated that these features of the conjugation band might arise from the large variety of structural situations present in the random structure compared to the alternating one.

P2 has a lower molecular weight than **P1**, and the ratio between electron rich/electron poor rings in the chain is comparable to **P1** (4.98 vs. 4.75). However, the perfect



Scheme 3 Structure of fluorene/thiophene (F–T) and fluorene/benzothiadiazole (F–B) alternating copolymers

alternation between 5- and 6-membered rings along the chain favors the planarity of the structure. As a consequence, the absorption is shifted to lower energy; in fact, the red band of **P2** (possibly due to a transition to a charge transfer state where the excited electron are localized on the benzothiadiazole electron-poor unit and the hole remains delocalized on fluorene and thiophene units [48]) is situated at 551 nm. The absorption edge is at 665 nm, corresponding to an optical gap of 1.86 eV.

Figure 3 shows the emission spectrum of **P1** excited at 460 nm. The photoluminescence of **P1**/PCBM blends in the solid state are also reported for various weight ratios. The PL intensity of **P1** is sharply reduced (30 times) by addition of about 10% w/w of PCBM, and almost two order of magnitude by addition of about 50% w/w of PCBM; a further increase in PCBM quantities (100% w/w) leads to no significant changes in PL quenching. This finding demonstrates that the electron transfer efficiency from the photoexcited polymer to the fullerene acceptor, and thus the photoluminescence quenching, increases with the PCBM concentration, suggesting that **P1** might be an effective polymer donor for solar cells. Similar conclusions apply to **P2** (Fig. 4), which is even more promising than **P1** for photovoltaic applications, thanks to its lower energy gap.

The LESR of films of the pristine polymers and 1:1 blends with PCBM are reported in Fig. 5. Concerning the pure polymer films a (weak) photoinduced signal is observed only on **P2**, at $g = 2.002$ and is assigned to photoinduced polarons P^{+o}/P^{-o} on the base of comparison with $g(P^{+o}) = 2.002$ in poly(alkylthiophene)s [34] and at $g(P^{+o}) = 2.003$ in poly(9,9-dioctylfluorene) [35]. Polaron

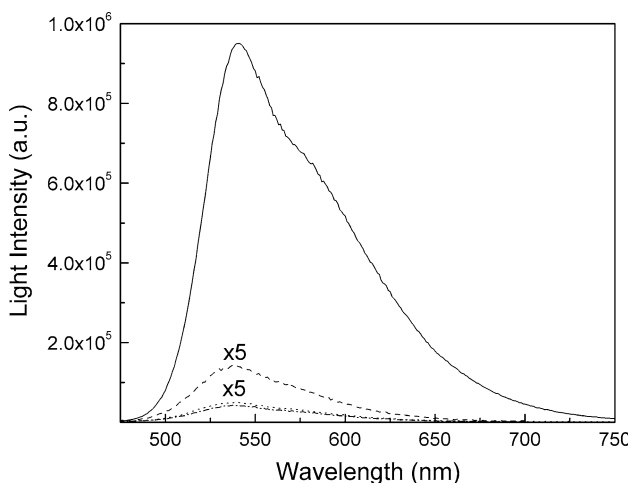


Fig. 3 Emission spectrum of pristine film of **P1** and PL quenching of polymer by PCBM in blend polymer:PCBM (1:0.1 w/w) (dash curve), (1:0.5 w/w) (dot curve), (1:1 w/w) (dash-dot curve). Excitation at 460 nm

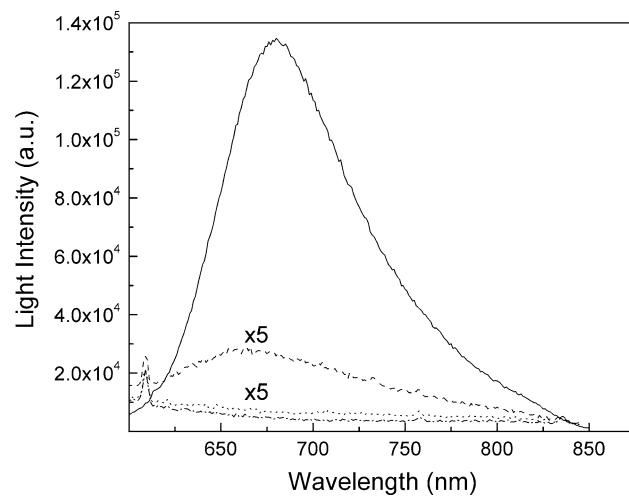


Fig. 4 Emission spectrum of pristine film of **P2** and PL quenching of polymer by PCBM in blend polymer:PCBM (1:0.1 w/w) (dash curve), (1:0.5 w/w) (dot curve), (1:1 w/w) (dash-dot curve). Excitation at 560 nm

formation is presumably due to charge transfer occurring between adjacent polymer chains or also in an intramolecular process, between electron rich and electron poor moieties. No polaron signal is observed in polymer **P1**, where photoexcitation is more likely relaxed through an intramolecular radiative decay, as shown by its strong fluorescence. In blends of both polymers with PCBM the polaron formation is photoinduced together with an absorption at $g = 1.999$ due to the fullerene anion [34]. This indicates the occurrence of some photoinduced charge transfer from the polymers towards the fullerene molecule. The higher concentration of photoinduced charges is observed in **P2**. The comparison of relative intensities shows that in the examined materials the photo-excited spin concentration is much lower than in reference poly(alkylthiophene):PCBM systems, similarly to what is reported also for poly(9,9-dioctylfluorene):PCBM blend [35]. Note, however, that the ESR signal is due to the equilibrium population of ESR active species over 10 μ s integration due to the detection at 100 kHz modulation, so that the contribution of very quickly recombining charges is lost. Therefore, the failure in observing an intense LESR spectrum of trapped charge species does not mean that the charge transfer has not occurred, but that the equilibrium population of charge transfer state is low, either because of weak generation or as an effect of strong recombination. From this point of view there is not any contradiction with fluorescence results on this same system, showing efficient quenching of emission upon PCBM addition; evidences from LESR suggest that in these systems there may be strong charge recombination.

Voltammetric analysis of **P1** and **P2** is reported in Fig. 6 and Table 2.

Fig. 5 LESR of pristine polymer films (**a**) and polymer:PCBM 1:1 w/w blend films (**b**). $T = 120$ K, microwave power = 0.05 mW, ≈ 2 mW/cm 2 irradiation from a high pressure Xenon lamp

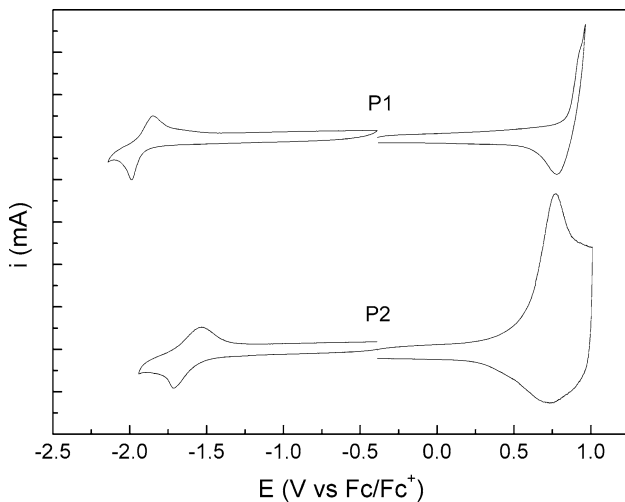
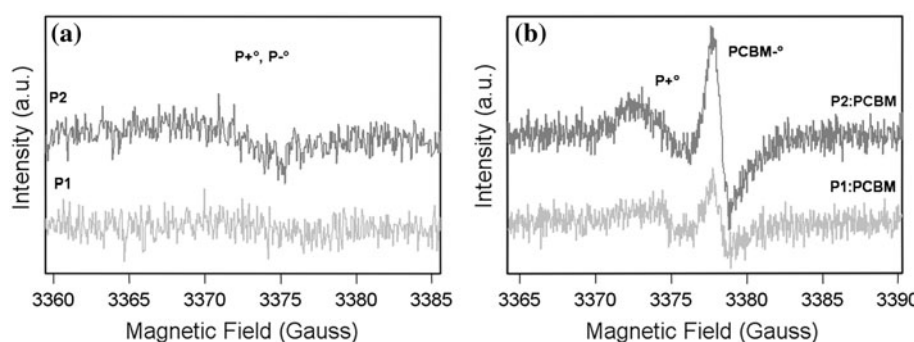


Fig. 6 CV of **P1** and **P2** in ACN + 0.1 M Bu₄NBF₄ on glassy carbon electrode vs. SCE at 0.2 V s $^{-1}$

In the cathodic zone, **P1** and **P2** voltammetric curves exhibit chemically reversible reduction behavior. The reduction onsets potential is more negative for **P1** than for **P2**, a behavior accounting for the fact that the copolymer (**P1**) with the higher content of electron rich units (F) has the lowest electron affinity.

In the anodic zone, the oxidation behavior of **P1** and **P2** is chemically reversible. The oxidation potentials is more positive for **P1** than for **P2** (>0.3 vs. Fc $^+$ /Fc), according with the donor character of this type of conjugated polymer and consistently with the ionization potentials expected on the basis of the balance of electron rich/electron poor groups.

The distance between first oxidation and reduction peak is not rigid, but is larger for **P1** which contains electron rich groups. This evidence suggests that the incipient radical cation and anion are differently delocalized on the conjugated system. Furthermore, molecular geometry and conjugation affect the electrochemical bandgap. In **P1** the loss of planarity, and consequently the loss in conjugation, could be another reason of difficult oxidation and reduction.

Table 2 Electrochemical properties of **P1–P2** copolymers (onset potentials vs. Fc/Fc $^+$), frontier energy levels ($E_{\text{HOMO(EC)}}$ and $E_{\text{LUMO(EC)}}$) and electrochemical gap ($E_{g(\text{EC})}$)

Entry	$E_{\text{onset}}^{\text{OX}}$ (V)	$E_{\text{onset}}^{\text{RED}}$ (V)	$E_{\text{HOMO(EC)}}$ (eV)	$E_{\text{LUMO(EC)}}$ (eV)	$E_{g(\text{EC})}$ (eV)
P1	0.81	-1.93	-5.61	-2.87	2.74
P2	0.51	-1.54	-5.31	-3.26	2.05

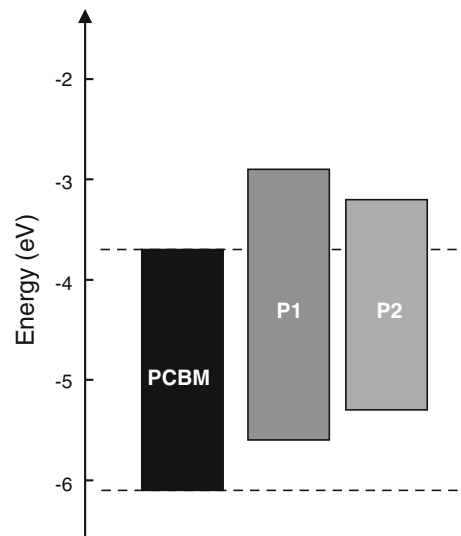


Fig. 7 Energy level diagram of **P1** and **P2** from voltammetric data. PCBM values are taken from the literature [50]

The HOMO and LUMO levels, calculated from the onsets of oxidation and reduction potentials according to the semi-empirical equations $E_{\text{HOMO/LUMO}} = [-e(E_{\text{onset(vs.SCE)}} - E_{\text{onset(Fc/Fc+ vs. SCE)}})] - 4.8$ eV [49] are reported in Table 2 and visually compared with the energy levels of PCBM [50] in Fig. 7.

For these two polymers the electrochemical gap is greater than the optical gap calculated from the absorption edges of UV-vis spectra (Table 1). This difference is commonly found in the literature [51] and is related to the formation of charge carriers in voltammetric analysis,

which requires higher energy than optical absorption. As a further observation, although great caution must be used when comparing electrochemical data from different laboratories, one can note that the HOMO level of **P2** (-5.31 eV) is about 0.2 eV higher in energy than the HOMO level of the corresponding F-T-B-T alternating copolymer (-5.5 [29]/ -5.56 [52] eV), whereas the gap is similar.

All the polymers have HOMO and LUMO levels higher than the commonly used PCBM acceptor (Fig. 7). **P1** is the polymer with the highest $E_{\text{HOMO} \text{donor}} - E_{\text{LUMO} \text{acceptor}}$ difference. On this basis [53], **P1** is expected to lead to PV devices with the better Voc. The $E_{\text{HOMO} \text{donor}} - E_{\text{LUMO} \text{acceptor}}$ difference of **P2** is lower, but the smaller energy gap could compensate the expected lower Voc with a higher Jsc in affording efficient solar cells.

Conclusions

In summary, three new pseudo-random conjugated copolymers, where in turn each fluorene, thiophene, benzothiadiazole comonomer unit is alternated to the other two units—which are randomly distributed—have been prepared by Suzuki polycondensation. The copolymers have been carefully purified to reduce the amount of residual catalyst (palladium) below 100 ppm. It was found that high molecular weights can be achieved for the structure which contains in high concentration monomer units bearing alkyl chains, which enhance the polymer solubility. When the polymer is not soluble enough (i.e., **P3**), it is not possible to reach high molecular weights because the material begins to precipitate from the reaction mixture in the early stages of polymerization.

UV-visible and voltammetric measurements show that the energy gaps vary according to the amount of electron poor-units in the chain: the polymer with alternating fluorene units (**P1**) exhibits the highest gap; the polymer with alternating thiophene units (**P2**) has the lowest gap. Both polymers are photoluminescent and the PL quenched by PCBM; under irradiation from a high pressure xenon lamp in order to simulate solar light spectrum photoexcited charge transfer is observed (in **P2** more than in **P1**), suggesting that they might act as donor materials for organic solar cells, in particular **P2**, matching both morphological and electronic requirements.

The optical and electronic properties of **P2**, that can be easily obtained starting from commercially available monomers, do not differ significantly from those of the corresponding perfectly alternating polymer, thus paving the way to the preparation of materials useful for photovoltaic application in a much more simplified manner.

Acknowledgement The authors are grateful to A. Oldani (ENI SpA) for molecular weights determinations, S. Perucchini and A. Congiu (ENI SpA) for elemental analysis and Prof. P. Mussini (University of Milano) for helpful discussion on voltammetric experiments.

References

1. Po R, Maggini M, Camaiori N (2010) *J Phys Chem C* 114:695
2. Kroon R, Lenes M, Hummelen JC, Blom PWM, De Boer B (2008) *Polym Rev* 48:531
3. Brabec CJ, Dyakonov V, Scherf U (2008) *Organic photovoltaics. Materials, device physics and manufacturing technologies*. Wiley-VCH, Weinheim
4. Chen J, Cao Y (2009) *Acc Chem Res* 42:1709
5. Liang Y, Feng D, Wu Y, Tsai ST, Li G, Ray C, Yu L (2009) *J Am Chem Soc* 131:7792
6. Chen HY, Hou J, Zhang S, Liang Y, Yang G, Yang Y, Yu L, Wu Y, Li G (2009) *Nat Photon* 3:649
7. Liang Y, Xu Z, Xia J, Tsai ST, Wu Y, Li G, Ray C, Yu L (2010) *Adv Mater* 22:E135
8. Scharber MC, Mühlbacher D, Koppe M, Denk P, Waldauf C, Heeger AJ, Brabec CJ (2006) *Adv Mater* 18:789
9. Sun S, Fan Z, Wang Y, Haliburton J (2005) *J Mater Sci* 40:1429. doi:[10.1007/s10853-005-0579-x](https://doi.org/10.1007/s10853-005-0579-x)
10. Janssen RAJ, Hummelen JC, Sariciftci NS (2005) *MRS Bull* 30:33
11. Karikomi M, Kitamura C, Tanaka S, Yamashita Y (1995) *J Am Chem Soc* 117:6791
12. van Mullekom HAM, Vekemans JAJM, Meijer EW (1998) *Chem Eur J* 4:1235
13. Hou Q, Xu Y, Yang W, Yuan M, Peng J, Cao Y (2002) *J Mater Chem* 12:2887
14. Berlin A, Zotti G, Zecchin S, Schiavon G, Vercelli B, Zanelli A (2004) *Chem Mater* 16:3667
15. Yang R, Tian R, Yan J, Zhang Y, Yang J, Hou Q, Yang W, Zhang C, Cao Y (2005) *Macromolecules* 38:244
16. Zhu Z, Waller D, Gaudiana R, Morana M, Mühlbacher D, Scharber M, Brabec CJ (2007) *Macromolecules* 40:1981
17. Beaujuge PM, Subbiah J, Choudhury KR, Ellinger S, McCarley TD, So F, Reynolds JR (2010) *Chem Mater* 22:2093
18. Zhou H, Yang L, Stoneking S, You W (2010) *ACS Appl Mater Interfaces* 2:1377
19. Svensson M, Zhang F, Inganäs O, Andersson MR (2003) *Synth Met* 135–136:137
20. Svensson M, Zhang F, Veenstra SC, Verhees WJH, Hummelen JC, Kroon JM, Inganäs O, Andersson MR (2003) *Adv Mater* 15:988
21. Inganäs O, Svensson M, Zhang F, Gadisa A, Persson NK, Wang X, Andersson MR (2004) *Appl Phys A* 79:31
22. Persson NK, Sun M, Kjellberg P, Pullerits T, Inganäs O (2005) *J Chem Phys* 123:204718
23. Ashraf RS, Hoppe H, Shahid M, Gobsch G, Sensfuss S, Klemm E (2006) *J Polym Sci A* 44:6952
24. Ashraf RS, Shahid M, Klemm E, Al-Ibrahim M, Sensfuss S (2006) *Macromol Rapid Commun* 27:1454
25. Admassie S, Inganäs O, Mammo W, Perzon E, Andersson MR (2006) *Synth Met* 156:614
26. Gadisa A, Mammo W, Andersson M, Admassie S, Zhang F, Andersson MR, Inganäs O (2007) *Adv Funct Mater* 17:3836
27. Slooff LH, Veenstra SC, Kroon JM, Moet DJD, Sweelssen J, Koetse MM (2007) *Appl Phys Lett* 90:143506
28. Gadisa A, Zhang F, Sharma D, Svensson M, Andersson MR, Inganäs O (2007) *Thin Solid Films* 515:3126

29. Chen MH, Hou J, Hong Z, Yang G, Sista S, Chen LM, Yang Y (2009) *Adv Mater* 21:4238
30. Li J, Osasa T, Hirayama Y, Sano T, Wakisaka K, Matsumura M (2007) *Sol Energy Mat Sol Cells* 91:745
31. Herland A, Thomsson D, Mirzov O, Scheblykin IG, Inganäs O (2008) *J Mater Chem* 18:126
32. Gritzner G, Kuta J (1984) *Pure Appl Chem* 56:461
33. Dyakonov V, Zorinians G, Scharber M, Brabec CJ, Janssen RAJ, Hummelen JC, Sariciftci NS (1999) *Phys Rev B* 59:8019
34. Marumoto K, Takeuchi N, Ozaki T, Kuroda S (2002) *Synth Met* 129:239
35. Marumoto K, Kato M, Kondo H, Kuroda S, Greenham NC, Friend RH, Shimoji Y, Abe S (2009) *Phys Rev B* 79:245204
36. Schläter AD (2001) *J Polym Sci A* 39:1533
37. Kirschbaum T, Briechn CA, Bäuerle PJ (2000) *J Chem Soc Perkin Trans* 1:1211
38. Gronowitz S, Bobosik V, Lawitz K (1984) *Chem Scr* 23:120
39. Forster M, Annan KO, Scherf U (1999) *Macromolecules* 32:3159
40. Jayakannan M, van Dongen JLJ, Janssen RAJ (2001) *Macromolecules* 34:5386
41. Perzon E, Zhang F, Andersson M, Mammo W, Inganäs O, Andersson MR (2007) *Adv Mater* 19:3308
42. Müller C, Wang E, Andersson LM, Tvingstedt K, Zhou Y, Andersson MR, Inganäs O (2010) *Adv Funct Mater* 20:2124
43. Björklund N, Lill JO, Rajander J, Österbacka R, Tierney S, Heeney M, McCulloch I, Cölle M (2009) *Org Electron* 10:215
44. Sonar P, Grimsdale AC, Heeney M, Shkunov M, McCulloch I, Müllen K (2007) *Synth Met* 157:872
45. Bijleveld JC, Shahid M, Gilot J, Wienk MM, Janssen RAJ (2009) *Adv Funct Mater* 19:3262
46. Hellström S, Zhang F, Inganäs O, Andersson MR (2009) *Dalton Trans* 2009:10032
47. Moses D, Dogariu A, Heeger AJ (2000) *J Phys Rev B* 61:9373
48. Jespersen KG, Beenken WJD, Zaushitsyn Y, Yartsev A, Andersson M, Pullerits T, Sundstrom V (2004) *J Chem Phys* 121:12613
49. Hwang SW, Chen Y (2001) *Macromolecules* 34:2981
50. Brabec CJ, Sariciftci NS, Hummelen JC (2001) *Adv Funct Mater* 11:15
51. Johansson T, Mammo W, Svensson M, Andersson MR, Inganäs O (2004) *J Mater Chem* 13:1316
52. Zhou E, Cong J, Yamakawa S, Wei Q, Nakamura M, Tajima K, Yang C, Hashimoto K (2010) *Macromolecules* 43:2873
53. Brabec CJ, Cravino A, Meissner D, Sariciftci NS, Fromherz T, Rispens MT, Sanchez L, Hummelen JC (2001) *Adv Funct Mater* 11:374